Published in final edited form as:

J Phys Chem Lett. 2018 May 03; 9(9): 2175–2180. doi:10.1021/acs.jpclett.8b00751.

Truncated Cross Effect Dynamic Nuclear Polarization: An Overhauser Effect Doppelgänger

Asif Equbal[†,§], **Yuanxin Li**[†,§], **Alisa Leavesley**[†], **Shengdian Huang**[‡], **Suchada Rajca**[‡], **Andrzej Rajca**[‡], and **Songi Han**[†,¶]

[†]Department of Chemistry and Biochemistry, University of California, Santa Barbara, Santa Barbara, California 93106, United States.

[‡]Department of Chemistry, University of Nebraska, Lincoln, Nebraska 68588-0304, United States.

[¶]Department of Chemical Engineering, University of California, Santa Barbara, Santa, Barbara, California 93106, United States.

Abstract

The discovery of a truncated cross-effect in dynamic nuclear polarization (DNP) NMR that has the features of an Overhauser-effect DNP (OE-DNP) is reported here. The apparent OE-DNP, where minimal μw-power achieved optimum enhancement, was observed when doping Trityl-OX063 with a proline nitroxide radical that possesses electron withdrawing, tetracarboxylate substituents (tetracarboxylate-ester-proline or TCP) in vitrified water/glycerol at 6.9 T and at 3.3 to 85 K, in apparent contradiction to expectations. While the observations are fully consistent with OE-DNP, we discover that a truncated cross-effect (*t*CE) is the underlying mechanism, owing to TCP's shortened T_{1e}. We take this observation as a guideline, and demonstrate that a crossover from CE to *t*CE can be replicated by simulating CE of a narrow-line (Trityl-OX063) and a broad-line (TCP) radical pair, with a significantly shortened T_{1e} of the broad-line radical.

Graphical Abstract

[§]Contributed equally to this work

Supporting Information

The supporting information on experimental and numerical methods, frequency- and power-profiles and relaxation properties of the radicals under different experimental is available free of charge on the ACS publication website at DOI: XXX.

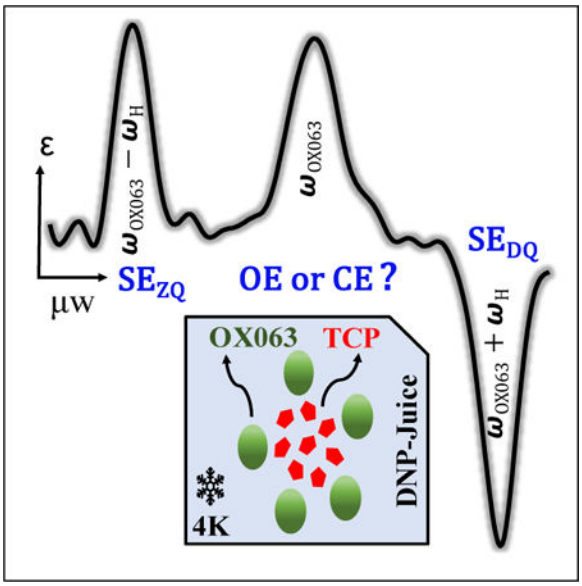

Dynamic nuclear polarization (DNP) is an important adjunct to nuclear magnetic resonance (NMR) to overcome its intrinsic insensitivity.[1–6] DNP enables magnetic resonance studies of a broad range of applications that would be infeasible otherwise, even at the highest available magnetic field. DNP exploits microwave-induced polarization transfer from unpaired electrons to nuclear spins, while three distinct DNP mechanisms are of main relevance: solid-effect (SE), cross-effect (CE), and Overhauser-effect (OE). Of these DNP mechanisms, SE and OE are straightforward to conceptualize, as they involve the direct transfer of polarization from an electron to a hyperfine-coupled nucleus. The optimal SE condition requires microwave (μw) irradiation at the forbidden electron-nuclear ($e-n$) double-quantum (DQ) and zero-quantum (ZQ) transitions.[7,8] The condition for OE is very different in that it requires w irradiation at the allowed single-quantum (SQ) transition as well as dynamics that render the $e-n$ ZQ and DQ cross-relaxation rates different. The CE mechanism involves two coupled electrons for transferring polarization to an unequally coupled nucleus.[9–12] The CE condition in an $e-e-n$ spin system is fulfilled when the difference in the resonance frequencies of the two electron spins equals the nuclear Larmor frequency.

An important focus in DNP has been on optimizing the paramagnetic polarizing-agent and solvent to yield maximum DNP enhancements under different mechanisms.[13–21] However, a rational understanding of the effect of the radical or radicals mixture, solvent, temperature, and magnetic fields on the DNP efficiency and mechanism is still elusive. The SE and CE are the most prominent DNP mechanisms in non-conducting solid-state samples. In contrast, the OE mechanism has been thought to be relevant only in conducting-solids or liquids, where electron spin-diffusion and molecular-tumbling motion can provide rapidly fluctuating hyperfine-couplings, causing efficient $e-n$ ZQ or DQ cross-relaxation.[1,2] However, contrary to expectations, Can *et. al.*[22] recently reported on an unexpected observation of OE with the non-conducting, narrow-line, polarizing-agent, 1,3-bisdiphenylene-2-phenylallyl (BDPA)[23] dispersed in polystyrene and with sulfonated-BDPA

(SA-BDPA)[24] in a glassy d8-glycerol/H_2O/D_2O (6:3:1, v/v/v) matrix termed DNP-juice, at ~100K and at magnetic fields between 5 and 18.8 T. This discovery of OE in insulating-solids is considered pivotal for the prospect of DNP in high magnetic fields, owing to the low μw-power requirement of OE and the potential field-independent DNP efficiency. However, the underlying relaxation mechanism in insulating solids is unknown, and therefore the mechanistic basis for the OE in insulating solids is inconclusive. This makes the discovery of OE in insulating-solids by Can *et. al.* unexpected and exciting. Even more curiously, reports of OE-DNP mechanism in non-conducting SA-BDPA have been made by Bodenhausen and coworkers at temperatures as low as 1.2 K under static conditions and at 6.7 T,[25] while there is no obvious physical basis for the occurrence of fast $e-n$ fluctuations near the electron Larmor frequency under these experimental conditions. Recent work by Pylaeva *et. al.*[26] discusses possible mechanisms for the observed OE in BDPA on the basis of molecular dynamics and spin dynamics simulations, but a rigorous experimental proof does not exist to date.

Counter to the proposed theory[26] and our own expectations, we observed very similar strong OE features with Trityl-OX063 (OX063) when doped with equivalent amounts of tetracarboxylate-ester-pyrroline (TCP) nitroxide radicals[27], a nitroxide radical that possesses electron withdrawing, gem-dicarboxylate ester substitutes, across a wide range of temperatures in DNP-juice. This intriguing discovery further showed that varying the solvent from DNP-juice to DMSO changed not only the DNP efficiency, but also the apparent DNP mechanism from OE to CE in hitherto unknown ways.

The structures of OX063 and the TCP radicals (TCP1 and TCP2) investigated here and their simulated EPR spectra at 6.9 T are shown in the SI (Fig. S2–3). From our preliminary testing, both TCP radicals display similar EPR parameters and DNP properties (SI, Fig. S3–5). The results shown here are mainly that of TPC2. This letter reports on a series of experiments and quantum mechanical calculations of the DNP mechanism that yield a rationale basis for the apparent OE observed with OX063-TCP mixtures in DNP-juice.

The DNP frequency-pro le is indicative of the underlying DNP mechanism and the optimum conditions.[6,9,28–30] Figure 1(a) shows the DNP frequency-pro le of a mixture containing 15 mM TCP2 and 15 mM OX063 in DNP-juice at 4 K. Significant ^{1}H DNP enhancements were observed at the μw irradiation frequencies of ~193.3 GHZ, ~193.6 GHz and ~193.9 GHz. Clearly, the enhancements at 193.3 GHz and 193.9 GHz are ±300 MHz apart from the OX063 center-frequency, and correspond to conditions for SE_{ZQ} and SE_{DQ} DNP, respectively. The enhancement at 193.6 GHz was *a priori* assigned to OE as it corresponds to OX063's center-frequency at 6.9 T. Observing OE around this frequency was not only unexpected, but also initially inexplicable, and therefore will be dubbed as OE* (till the time its actual origin is proven later), with the * denoting an apparent OE. Surprisingly, no visible features of DNP resulting from TCP2 in DNP-juice appeared in the observed frequency-profile.

The DNP frequency-profile was also measured for the same OX063-TCP2 mixture in DMSO. Adding to the OE* conundrum, the frequency-pro le in DMSO displayed a diametrically different frequency envelope compared to DNP-juice, revealing a dominant CE

mechanism. The positive and negative maximum enhancements were observed at ~193.6 GHz and ~193.9 GHz, respectively (Figure 1(b)). The separation of these maximum peak positions by 300 MHz is consistent with CE between OX063 and TCP2, while the broader features are presumably due to CE between two TCP2 radicals, where a range of electron spin pairs at different μw-frequencies fulfill the CE conditions. The presence of the OE* mechanism in DMSO cannot be ruled out, since the optimum frequency for the OE* (in DNP-juice) coincides with the peak resulting from TCP2-OX063 CE. At 193.6 GHz (optimum for OE*), enhancements (NMR signal intensity ratio: μw-power *on*/*of f*) of ~31 was observed for TCP2-OX063 in DNP-juice and ~139 in DMSO, both at 4 K with 120 mW μw-power and 60-s irradiation.

Next, the radical mixture composition was investigated to achieve optimum OE* enhancements in DNP-juice (at 4 K, 120 mW μw-power, 60-s μw-irradiation). The DNP frequency-profile of a series of TCP2/OX063 mixtures were recorded, where the OX063 con-centration was fixed at 15 mM and the TCP2 concentration varied from 0 to 60 mM (Figure 2(a)). All frequency-profiles were normalized with the optimum SE_{DQ} enhancement. The DNP frequency-pro les show OE* enhancements only with TCP2 doping, in addition to SE enhancements at 193.3 and 193.9 GHz. The absolute OE* enhancement and its relative efficiency with respect to SE_{DQ}, $\varepsilon_{OE*}/\varepsilon_{SE}{}_{DQ}$, are plotted in Figure 2(b). They show that an increase in the TCP2 concentration leads to an increase in the OE* enhancement up to 30 mM, after which it plateaus with increasing TCP2 concentration (and slightly decreases at 60 mM). For all the following investigations, the radical composition was fixed to the optimum composition of 15 mM OX063 and 30 mM TCP2.

The DNP power-curve (enhancement vs. μw-power) at the OE* frequency showed that the maximum enhancement (at 60 s μw-irradiation) was reached at merely 7 mW of μw-power, as shown in Figure 3(a). Remarkably, 90% of the maximum enhancement was achieved with minuscule (4 mW) w-power, further corroborating the signature properties of OE. In stark contrast, the optimum-power for SE-DNP enhancements could not be met by even 120 mW of μw-power. At low μw-power, the OE*-derived enhancement was higher by 16-fold compared to the SE-derived enhancements. At higher w-power (>70 mW), the SE began to dominate over the OE* (at 4 K). Impressively, the low-power requirement to saturate the OE* resonance was observed even at higher temperatures of 10 and 25 K, and at low TCP2 concentrations (5 mM), indicating that the OE* effect is not power limited under the tested conditions (SI, Fig. S7). The OE* phenomenon was observed across all the temperatures, from 3.3 to 85 K (SI, Fig. S6). The temperature dependent DNP-measurement showed a sharp increase in OE* enhancement below 5 K, indicating the pivotal role of electron relaxation in the OE* phenomenon, given that its saturation can be ruled out as a limiting factor.

Scrutinizing the OE* discovery, we first compare our results with reported OE studies of BDPA in the literature. Can *et. al.* attributed the absence of OE in OX063 and perdeuterated-BDPA (d_{21}-BDPA) to the absence of strong $e-H$ couplings.[22] In our case, OX063, all hydrogen atoms in the aromatic rings joined directly to the carbon radical center are purposefully substituted to remove the influence of large $e-H$ hyper ne-couplings.[14] The study by Pylaeva *et. al.*[26] further proposed that fluctuations in the electron spin-density in

BDPA results from conjugation in the carbon-radical position, leading to hyper ne-couplings fluctuations. Ji *et. al.*[25] hypothesized that stochastic motions at low vibration frequencies can be a source of non-zero spectral-density at the electron resonance frequency leading to cross-relaxation, effective at low temperatures. Hyperfine-coupling fluctuations due to conjugation would not be a plausible mechanism for OX063, as its radical-center is fixed. Therefore, OX063 does not meet any of the hypothesized requirements (strong $e-n$ coupling and conjugation) for exhibiting OE in the pure or doped-state. Equally peculiar is our observation that OE* is turned on/off with the choice of the glassing solvent. Although the results duplicate the apparent properties of OE-DNP observed in insulating-solids, it does not meet the proposed theoretical basis.

Solving this OE* riddle requires scrutiny of the electron spin dynamics. This was enabled with unique instrumentation, which allowed for EPR measurements, polarization-profile, and electron-relaxation times under the relevant DNP conditions.[31] The echo-detected T_{1e} relaxation rates were measured at the frequencies corresponding to OE* and SE transitions. The T_{1e} of pure OX063 in DNP-juice was found to be ~16 ms, which shortened to ~4 ms upon addition of 30 mM TCP2 (Figure 3(b)). Crucially, the T_{1e} of TCP2 in DNP-juice was too short to be detected which was also attributed to very short T_m, while T_{1e} of TCP2 in DMSO was significantly longer (~17 ms). This hints at clustering[32,33] of TCP2 in DNP-juice. This was confirmed by CW X-band EPR, where signatures of dipolar broadening were observed for TCP2 in DNP-juice, but not in DMSO (SI, Section2). That the T_{1e} of OX063 and/or nitroxide radicals are so critically solvent and mixture-dependent was unexpected, showcasing the need to evaluate T_{1e} at the precise experimental DNP conditions. Tabulated T_{1e} values and further discussions on T_{1e} with respect to literature can be found in the SI.

Further insight was gained with electron-electron double resonance (ELDOR) that measures how EPR saturation or polarization at one frequency is transferred to another frequency. In the ELDOR-pro le shown in Figure 3(c), the electron detection/probe frequency was set to that of the OX063 center, and the saturating/pump frequency was scanned from 193.5 to 193.75 GHz with 120 mW power at 4 K. The ELDOR-pro le showed that μw-irradiation resonant with TCP2 did not affect the OX063 resonance. This is consistent with the very fast relaxation of TCP2 in DNP-juice, which prevents it saturation by μw. Also, the hole burnt at the OX063 frequency narrows upon addition of TCP2, consistent with the shortening of OX063's T_{1e} upon doping with TCP2, especially with clustered TCP2 in DNP-juice.

Inspired by the observed EPR results, we quantum mechanically simulated the DNP frequency-pro le for a narrow radical (e_1-OX063) and a broad radical (e_2-TCP2), unequally coupled to a proton in an $e_1-e_2-{}^1H$ system. Mimicking the slow-fast relaxation rate combination observed in DNP-juice, T_{1e} of e_1 and e_2 were set to 4 and 0.01 ms, respectively. The DNP simulation was performed using Spin Evolution, a software package for spin dynamics simulations.[34] All relevant details of the simulation are provided in the SI. Remarkably, we could replicate the experimental ^1H enhancement frequency-profile of the OX063-TCP2 mixture. A positive maximum enhancement is observed at the OX063 center-frequency, as well as ±300 MHz apart from the OX063 center, representing the SE_{ZQ} and SE_{DQ} conditions. Clearly, the OE* feature is observed, even though the cross-relaxation mechanisms are turned off, i.e. the mechanistic prerequisites for OE are eliminated. This

shows that the observed OE* is just a **truncated CE** (*t*CE) induced by conditions when one of the two electron spins involved in the CE has a very short T_{1e}. The CE relies on the selective saturation of one of the coupled electron spins. Thus, irradiation of the slower relaxing, "*easy to saturate*", electron spin (e_1) (193.6 GHz in Fig. 4(b)) will lead to an effective polarization transfer to the nucleus. In contrast, irradiation of the very fast relaxing electron spin (e_2) will not result in electron saturation, and thus no appreciable polarization differential. Consequently, the CE polarization transfer will be truncated at the EPR frequencies resonant with the fast relaxing radical, TCP2 in this study.

In summary, this letter reports on the discovery of a truncated cross-effect (*t*CE) that has the appearance of an Overhauser-effect DNP. Such an effect was observed when doping OX063 with the nitroxide based radical, TCP2, in vitrified water/glycerol. The mechanistic basis for this astonishing effect was found to be a substructure of the CE mechanism defined by distinct electron spin dynamics properties of fast and slow relaxing radicals. The puzzling OE* or the *t*CE mechanism can be replicated by quantum mechanical simulations with a mixed radical system, where the two radicals maximize the EPR spectral overlap to fulfill the CE conditions, while one radical type is easily saturated, but not the other, due to very short T_{1e}. This discovery is potentially important in many different ways, one of which is the prospect of the *t*CE serving as an indirect read out of "dark" (or invisible) electron spins that, despite being undetectable, elicit a *t*CE by means of a detectable reporter radical. The OE characteristics may be a spurious effect owing to its similarity with the *t*CE, and therefore, probing the electron spins dynamics will be the ultimate test of the underlying mechanism, and not just analysis of the DNP frequency- and power- pro les.[35,36] We also clarify that our study cannot address the mechanistic basis of OE in BDPA, as it is impossible to differentiate between OE and *t*CE (OE' s doppelgänger) in the case of BDPA with the present level of theoretical understanding, and the currently available experimental methods. Accordingly, we opine that the proposed theory of OE in BDPA as well as the herein discovered *t*CE in doped OX063 can stand in parallel.

Supplementary Material

Refer to Web version on PubMed Central for supplementary material.

Acknowledgement

This work was supported by the National Science Foundation (NSF) (CHE #1505038 to SH and #CHE-1665256 to AR) and the National Institute of Health (NIH) (NIBIB #1R21EB022731 to SH and NIGMS #R01GM124310-01 to SR and AR). The content is solely the responsibility of the authors and does not necessarily represent the official views of the National Institutes of Health.

References

(1). Overhauser AW Polarization of nuclei in metals. Physical Review 1953, 92, 411.

(2). Carver TR; Slichter CP Polarization of nuclear spins in metals. Physical Review 1953, 92, 212.

(3). Wind R; Duijvestijn M; Van Der Lugt C; Manenschijn A; Vriend J Applications of dynamic nuclear polarization in 13C NMR in solids. Progress in Nuclear Magnetic Resonance Spectroscopy 1985, 17, 33–67.

(4). Ardenkjær-Larsen JH; Fridlund B; Gram A; Hansson G; Hansson L; Lerche MH; Servin R; Thaning M; Golman K Increase in signal-to-noise ratio of > 10,000 times in liquid-state NMR. Proceedings of the National Academy of Sciences 2003, 100, 10158–10163.

(5). Ardenkjaer-Larsen J-H; Boebinger GS; Comment A; Duckett S; Edison AS; Engelke F; Griesinger C; Griffin RG; Hilty C; Maeda H et al. Facing and over-coming sensitivity challenges in biomolecular NMR spectroscopy. Angewandte Chemie International Edition 2015, 54, 9162–9185. [PubMed: 26136394]

(6). Thankamony ASL; Wittmann JJ; Kaushik M; Corzilius B Dynamic nuclear polarization for sensitivity enhancement in modern solid-state NMR. Progress in Nuclear Magnetic Resonance Spectroscopy 2017, 102–103, 120 – 195.

(7). Jeffries C Polarization of nuclei by resonance saturation in paramagnetic crystals. Physical Review 1957, 106, 164.

(8). Hovav Y; Feintuch A; Vega S Theoretical aspects of dynamic nuclear polarization in the solid state–the solid effect. Journal of Magnetic Resonance 2010, 207, 176–189. [PubMed: 21084205]

(9). Hwang CF; Hill DA Phenomenological model for the new effect in dynamic polarization. Physical Review Letters 1967, 19, 1011.

(10). Hovav Y; Feintuch A; Vega S Theoretical aspects of dynamic nuclear polarization in the solid state–the cross effect. Journal of Magnetic Resonance 2012, 214, 29–41. [PubMed: 22119645]

(11). Thurber KR; Tycko R Theory for cross effect dynamic nuclear polarization under magic-angle spinning in solid state nuclear magnetic resonance: the importance of level crossings. The Journal of chemical physics 2012, 137, 084508. [PubMed: 22938251]

(12). Mentink-Vigier F; Akbey U; Oschkinat H; Vega S; Feintuch A Theoretical aspects of magic angle spinning-dynamic nuclear polarization. Journal of Magnetic Resonance 2015, 258, 102–120. [PubMed: 26232770]

(13). Song C; Hu K-N; Joo C-G; Swager TM; Griffin RG TOTAPOL: a biradical polarizing agent for dynamic nuclear polarization experiments in aqueous media. Journal of the American Chemical Society 2006, 128, 11385–11390. [PubMed: 16939261]

(14). Hu K-N; Bajaj VS; Rosay M; Griffin RG High-frequency dynamic nuclear polarization using mixtures of TEMPO and trityl radicals. The Journal of chemical physics 2007, 126, 044512. [PubMed: 17286492]

(15). Zagdoun A; Rossini AJ; Gajan D; Bourdolle A; Ouari O; Rosay M; Maas WE; Tordo P; Lelli M; Emsley L et al. Non-aqueous solvents for DNP surface enhanced NMR spectroscopy. Chemical Communications 2012, 48, 654–656. [PubMed: 22034623]

(16). Zagdoun A; Casano G; Ouari O; Lapadula G; Rossini AJ; Lelli M; Baffert M; Gajan D; Veyre L; Maas WE et al. A slowly relaxing rigid biradical for efficient dynamic nuclear polarization surface-enhanced NMR spectroscopy: expeditious characterization of functional group manipulation in hybrid materials. Journal of the American Chemical Society 2012, 134, 2284–2291. [PubMed: 22191415]

(17). Sauvée C; Rosay M; Casano G; Aussenac F; Weber RT; Ouari O; Tordo P Highly Efficient, Water-Soluble Polarizing Agents for Dynamic Nuclear Polarization at High Frequency. Angewandte Chemie International Edition 2013, 52, 10858–10861. [PubMed: 23956072]

(18). Mathies G; Caporini MA; Michaelis VK; Liu Y; Hu K-N; Mance D; Zweier JL; Rosay M; Baldus M; Griffin RG Efficient dynamic nuclear polarization at 800 MHz/527 GHz with trityl-nitroxide biradicals. Angewandte Chemie International Edition 2015, 54, 11770–11774. [PubMed: 26268156]

(19). Kubicki DJ; Casano G; Schwarzwälder M; Abel S; Sauvee C; Ganesan K; Yulikov M; Rossini AJ; Jeschke G; Coperet C et al. Rational design of dinitroxide biradicals for efficient cross-effiect dynamic nuclear polarization. Chemical Science 2016, 7, 550–558. [PubMed: 29896347]

(20). Perras FA; Reinig RR; Slowing II; Sadow AD; Pruski M Effects of biradical deuteration on the performance of DNP: towards better performing polarizing agents. Physical Chemistry Chemical Physics 2016, 18, 65–69. [PubMed: 26619055]

(21). Lelli M; Chaudhari SR; Gajan D; Casano G; Rossini AJ; Ouari O; Tordo P; Lesage A; Emsley L Solid-state dynamic nuclear polarization at 9.4 and 18.8 T from 100 K to room temperature. Journal of the American Chemical Society 2015, 137, 14558–14561. [PubMed: 26555676]

(22). Can TV; Caporini MA; Mentink-Vigier F; Corzilius B; Walish JJ; Rosay M; Maas WE; Baldus M; Vega S; Swager TM et al. Overhauser effects in insulating solids. The Journal of Chemical Physics 2014, 141, 064202. [PubMed: 25134564]

(23). Koelsch CF Syntheses with Triarylvinylmagnesium Bromides.,-Bisdiphenylene--phenylallyl, a Stable Free Radical. Journal of the American Chemical Society 1957, 79, 4439–4441.

(24). Haze O; Corzilius B; Smith AA; Griffin RG; Swager TM Water-Soluble Narrow-Line Radicals for Dynamic Nuclear Polarization. Journal of the American Chemical Society 2012, 134, 14287–14290. [PubMed: 22917088]

(25). Ji X; Can T; Mentink-Vigier F; Bornet A; Milani J; Vuichoud B; Caporini M; Griffin R; Jannin S; Goldman M et al. Overhauser effects in non-conducting solids at 1.2K. Journal of Magnetic Resonance 2018, 286, 138–142. [PubMed: 29241045]

(26). Pylaeva S; Ivanov KL; Baldus M; Sebastiani D; Elgabarty H Molecular Mechanism of Overhauser Dynamic Nuclear Polarization in Insulating Solids. The Journal of Physical Chemistry Letters 2017, 8, 2137–2142. [PubMed: 28445055]

(27). Huang S; Paletta JT; Elajaili H; Huber K; Pink M; Rajca S; Eaton GR; Eaton SS; Rajca A Synthesis and Electron Spin Relaxation of Tetracarboxylate Pyrroline Nitroxides. The Journal of Organic Chemistry 2017, 82, 1538–1544. [PubMed: 28032758]

(28). Banerjee D; Shimon D; Feintuch A; Vega S; Goldfarb D The interplay between the solid effect and the cross effect mechanisms in solid state 13C DNP at 95 GHz using trityl radicals. Journal of Magnetic Resonance 2013, 230, 212–219. [PubMed: 23522876]

(29). Ravera E; Shimon D; Feintuch A; Goldfarb D; Vega S; Flori A; Luchinat C; Menichetti L; Parigi G The effect of Gd on trityl-based dynamic nuclear polarisation in solids. Physical Chemistry Chemical Physics 2015, 17, 26969–26978. [PubMed: 26403358]

(30). Leavesley A; Shimon D; Siaw TA; Feintuch A; Goldfarb D; Vega S; Kaminker I; Han S Effect of electron spectral diffusion on static dynamic nuclear polarization at 7 Tesla. Physical Chemistry Chemical Physics 2017, 19, 3596–3605. [PubMed: 28094364]

(31). Siaw TA; Fehr M; Lund A; Latimer A; Walker SA; Edwards DT; Han S-I Effect of electron spin dynamics on solid-state dynamic nuclear polarization performance. Physical Chemistry Chemical Physics 2014, 16, 18694–18706. [PubMed: 24968276]

(32). Olankitwanit A; Kathirvelu V; Rajca S; Eaton GR; Eaton SS; Rajca A Calix [4] arene nitroxide tetraradical and octaradical. Chemical Communications 2011, 47, 6443–6445. [PubMed: 21541435]

(33). Sato H; Kathirvelu V; Spagnol G; Rajca S; Rajca A; Eaton SS; Eaton GR Impact of Electron-Electron Spin Interaction on Electron Spin Relaxation of Nitroxide Diradicals and Tetraradical in Glassy Solvents Between 10 and 300 K. The Journal of Physical Chemistry B 2008, 112, 2818–2828. [PubMed: 18284225]

(34). Veshtort M; Griffin RG SPINEVOLUTION: a powerful tool for the simulation of solid and liquid state NMR experiments. Journal of Magnetic Resonance 2006, 178, 248–282. [PubMed: 16338152]

(35). Hovav Y; Shimon D; Kaminker I; Feintuch A; Goldfarb D; Vega S Effects of the electron polarization on dynamic nuclear polarization in solids. Physical Chemistry Chemical Physics 2015, 17, 6053–6065. [PubMed: 25640165]

(36). Hovav Y; Kaminker I; Shimon D; Feintuch A; Goldfarb D; Vega S The electron depolarization during dynamic nuclear polarization: measurements and simulations. Physical Chemistry Chemical Physics 2015, 17, 226–244. [PubMed: 25384575]

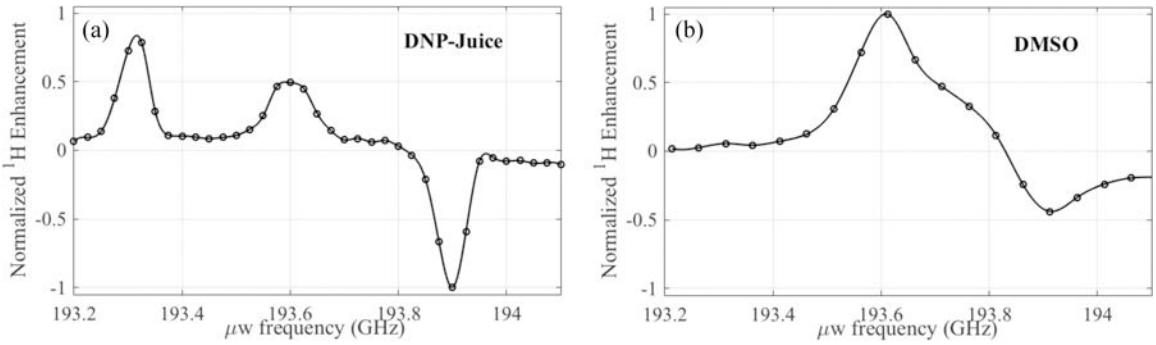

Figure 1:

DNP frequency pro les of 15 mM TCP2 – 15 mM OX063 mixture at 4 K in (a) DNP-juice; (b) DMSO. DNP frequency-profiles were obtained by measuring ^{1}H DNP signal enhancement as a function of μw irradiation frequency which was swept from 193.2 GHz to 194.1 GHz, with 120 mW μw-power and 60 s irradiation time. The ^{1}H enhancements displayed were normalized by the maximum absolute value.

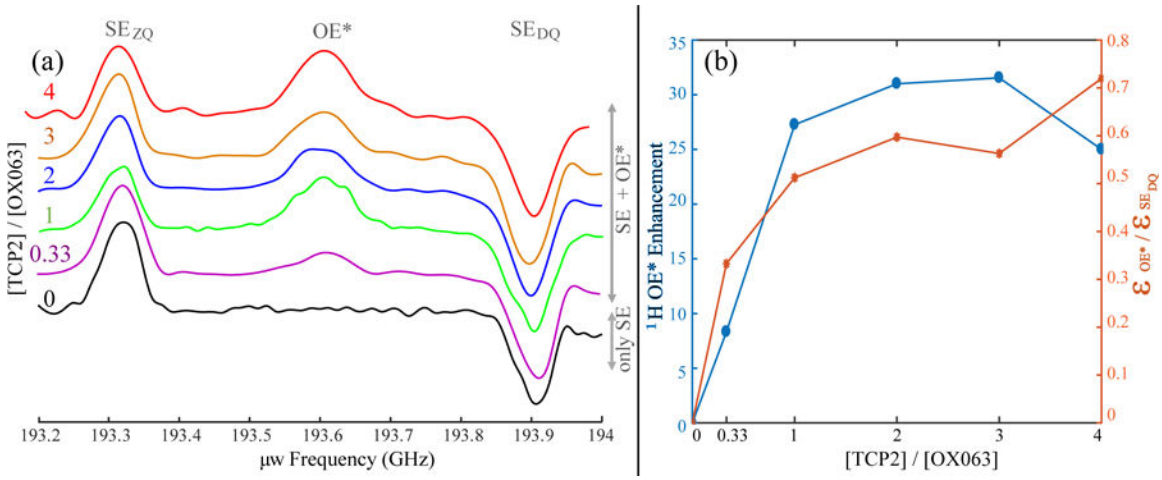

Figure 2:

(a) TCP2:OX063 ratio optimization for maximum OE* enhancement at 4 K in DNP-juice using: 60 s μw irradiation time and 120 mW μw-power. OX063 concentration was fixed to 15 mM. All the pro les are normalized to the corresponding SE_{DQ} enhancement number. (b) Absolute OE* enhancement is plotted on the left y-axis and $\varepsilon_{OE*}/\varepsilon_{SEDQ}$ ratio is plotted on the right y-axis for different radical concentrations.

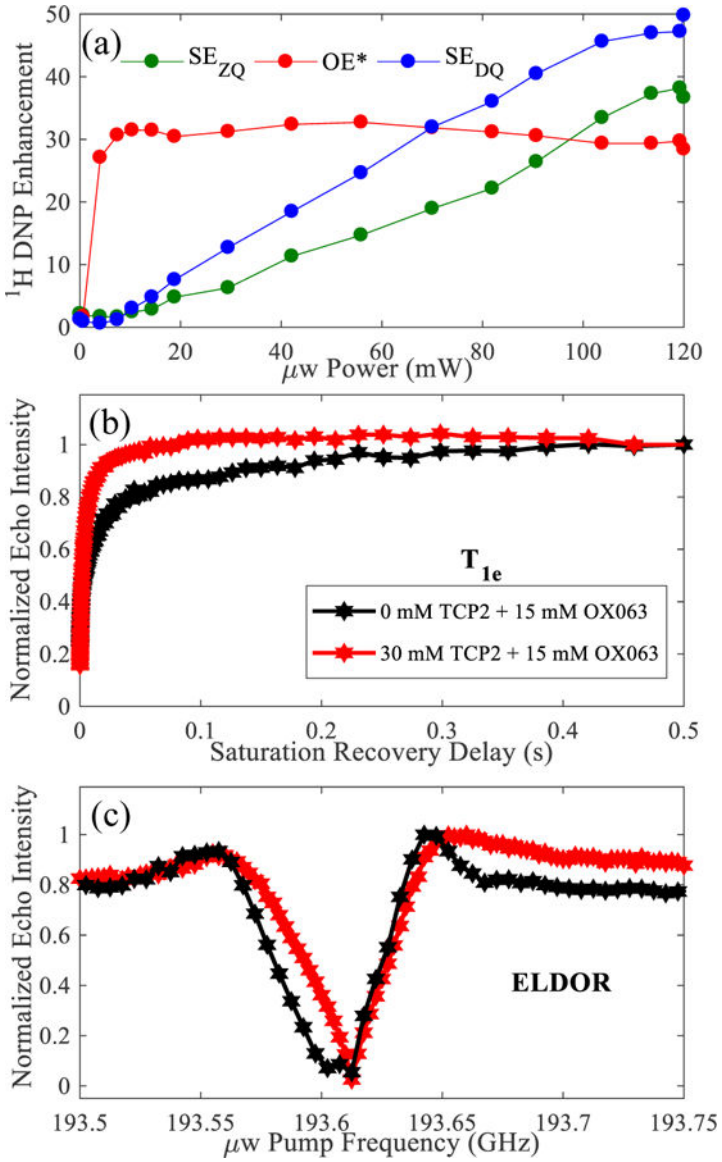

Figure 3:

(a) DNP power saturation experiments of 15 mM OX063 30 mM TCP2 mixture in DNP-juice recorded at 4 K with μw-power varied from 0 to 120 mW and 60 s μw-irradiation. The μw-frequency was fixed at the optimum conditions for SE_{ZQ} (green), OE* (red) and SE_{DQ} (blue), respectively. (b) T_{1e} of pure OX063 (black) and TCP2-doped OX063 (red) at 4 K. (c) ELDOR of pure OX063 (black) and TCP2-doped OX063 (red) at 4 K.

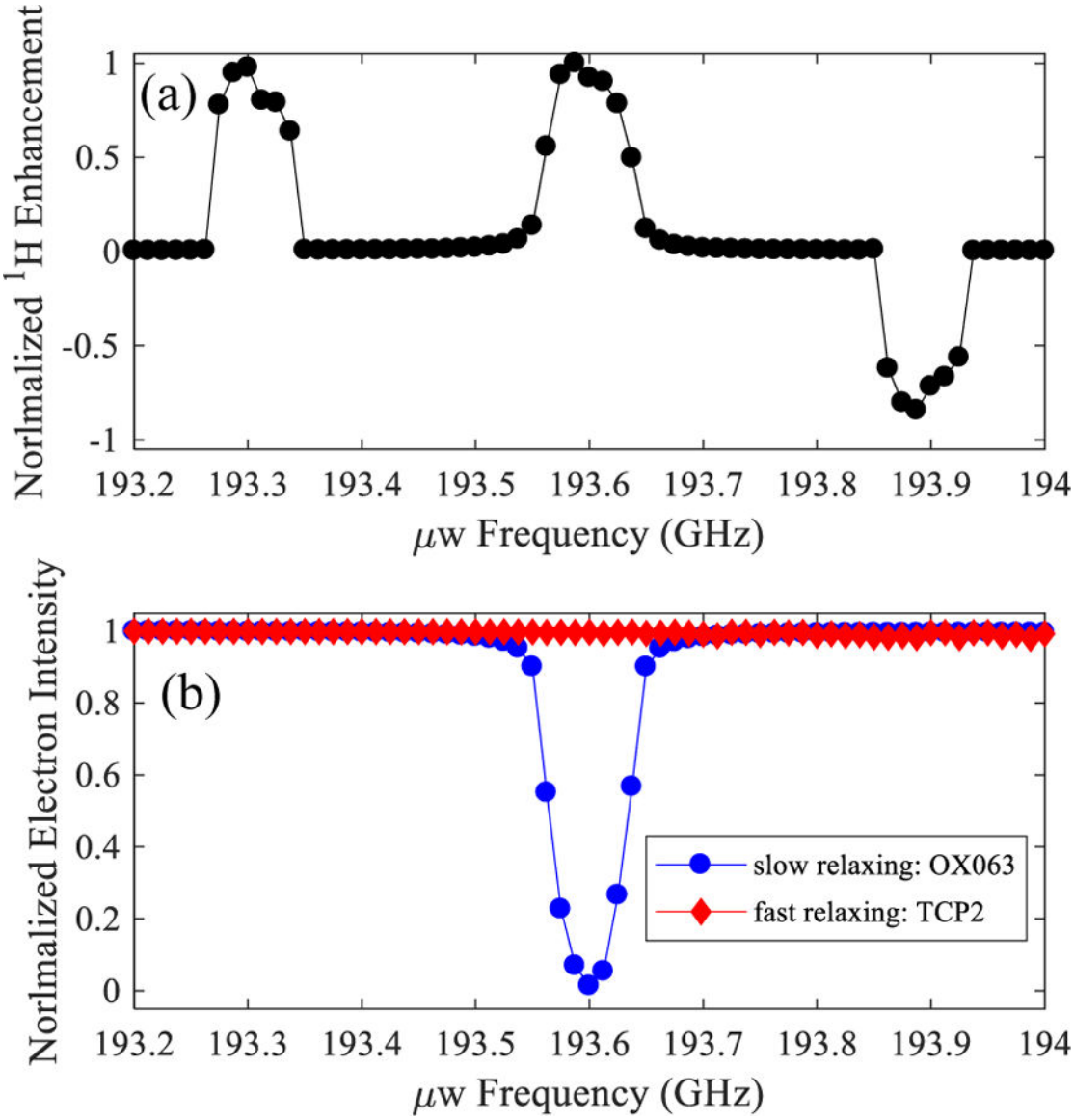

Figure 4:

(a) Simulated ^{1}H DNP enhancement as a function of μw irradiation frequency, for a $e - e - ^1$H spin system at 300 MHz conditions. (b) Polarization measurements of the two electrons under the DNP conditions of figure 1(a). This is demonstrated using a three spins (two electrons and one proton) based simulation at the experimental condition taken of figure 1. The longitudinal relaxation rate constants of electrons are taken to be 0.01 and 4 ms, mimicking relaxation rates of TCP2 and OX063, respectively. All the other simulation parameters are mentioned in the supporting information (SI, Section3).